UCLA
UCLA Previously Published Works

Title

Activation of MAPK Signaling by CXCR7 Leads to Enzalutamide Resistance in Prostate Cancer

Permalink

Journal

ISSN

Authors

Li, Shangze
Fong, Ka-wing
Gritsina, Galina
et al.

Publication Date

DOI

Peer reviewed

Activation of MAPK signaling by CXCR7 leads to enzalutamide resistance in prostate cancer

Shangze Li[1,*], **Ka-wing Fong**[1,*], **Galina Gritsina**[1], **Ali Zhang**[1], **Jonathan C. Zhao**[1], **Jung Kim**[1], **Adam Sharp**[2,3], **Wei Yuan**[2], **Caterina Aversa**[2,3], **Ximing J. Yang**[4,10], **Peter S. Nelson**[5], **Felix Y. Feng**[6], **Arul Chinnaiyan**[7], **Johann S. de Bono**[2,3], **Colm Morrissey**[8], **Matthew B. Rettig**[9], and **Jindan Yu**[1,10]

[1]Division of Hematology/Oncology, Department of Medicine, Northwestern University Feinberg School of Medicine, Chicago, IL, USA;

[2]Institute of Cancer Research, London, United Kingdom

[3]Royal Marsden Hospital, London, United Kingdom

[4]Department of Pathology, Northwestern University, Chicago, Illinois.

[5]Division of Human Biology, Fred Hutchinson Cancer Research Center, Seattle, Washington.

[6]Departments of Radiation Oncology, Urology, and Medicine, Helen Diller Family Comprehensive Cancer Center, University of California San Francisco, San Francisco, California.

[7]Michigan Center for Translational Pathology, University of Michigan, Ann Arbor, Michigan 48109, USA.

[8]Department of Urology, University of Washington, Seattle, Washington.

[9]Department of Medicine, Division of Hematology-Oncology, David Geffen School of Medicine at UCLA, Los Angeles, CA, 90095, USA and VA Greater Los Angeles Healthcare System, Los Angeles, CA 90073, USA.

[10]Robert H. Lurie Comprehensive Cancer Center, Northwestern University, Chicago, IL, USA

Abstract

Castration-resistant prostate cancer (CRPC) that has developed resistance to the new-generation androgen receptor (AR) antagonist enzalutamide is a lethal disease. Transcriptome analysis of multiple prostate cancer models identified CXCR7, an atypical chemokine receptor, as one of the most upregulated genes in enzalutamide-resistant cells. AR directly repressed CXCR7 by binding to an enhancer 110kb downstream of the gene and expression was restored upon androgen deprivation. We demonstrate that CXCR7 is a critical regulator of prostate cancer sensitivity to

Address correspondence and requests for reprints to: Jindan Yu, Ph.D., Division of Hematology/Oncology, Department of Medicine, Robert H. Lurie Comprehensive Cancer Center, Northwestern University, Feinberg School of Medicine, 303 E. Superior St. Lurie 5-117, Chicago, IL 60611, Phone: 312-503-1761, jindan-yu@northwestern.edu.
*These authors contributed equally to this work.

enzalutamide and is required for CRPC growth in vitro and in vivo. Elevated CXCR7 activated MAPK/ERK signaling through ligand-independent but β-arrestin 2-dependent mechanisms. Examination of patient specimens showed that CXCR7 and pERK levels increased significantly from localized prostate cancer to CRPC and further upon enzalutamide resistance. Preclinical studies revealed remarkable efficacies of MAPK/ERK inhibitors in suppressing enzalutamide-resistant prostate cancer. Overall, these results indicate that CXCR7 may serve as a biomarker of resistant disease in patients with prostate cancer and that disruption of CXCR7 signaling may be an effective strategy to overcome resistance.

Keywords

Androgen receptor; ACKR3; ERK phosphorylation; β-arrestin 2 or ARRB2; CXCL12 /SDF-1α chemokine; MEK inhibitor Trametinib; ChIP-seq; RNA-seq

Introduction

The androgen receptor (AR) is a major driver of the growth of prostate cancer (PCa) (1,2) and aberrant AR signaling remains to play major roles in final-stage castration-resistant prostate cancer (CRPC) that have developed resistance to the second-generation AR antagonist enzalutamide (Enz), or the androgen-biosynthesis inhibitor abiraterone acetate (3–7). Further, elevated expression of the glucocorticoid receptor can bypass dependence on the AR by promiscuously activating AR target genes (8) or through lineage plasticity driven by SOX2 (9). Clearly, there are multiple escape pathways to Enz resistance, and a comprehensive understanding of these underlying mechanisms is critical for identifying novel therapeutic targets to improve CRPC outcomes.

The chemokines and chemokine receptors play important roles in chemotaxis, inflammation, and cancer dissemination. CXCR7 is an atypical chemokine receptor (ACKR3), as it functions through G-protein-independent mechanisms. Activated CXCR7 interacts with β-arrestin 2 (ARRB2) and the complex internalizes into clathrin-coated endosomes within the cells and recruits MAPK proteins for the phosphorylation of ERK1/2 (10). Although able to bind CXCL12 (also called SDF-1α), CXCR7 has been shown to be constitutively active in some cells including breast cancer cells, demonstrating ligand-independent activation (11). CXCR7 expression was detected in PCa (12), and emerging evidence suggests important roles of CXCR7 in prostate tumorigenesis (13–15). Here we identify *CXCR7* as a top up-regulated gene in Enz-resistant PCa and demonstrate important roles of CXCR7/ MAPK/ERK signaling in driving PCa resistance to Enz.

Material and Methods

Cell culture, Constructs, and Reagents

LNCaP, VCaP and HEK293T cell lines were obtained from the ATCC. To authenticate the cells, LNCaP and VCaP cells were subjected to short tandem repeat DNA profiling (Genetica) in February of 2017, and subsequently the amplified DNA sequences were compared to reference cell database. Only percent match >80% was regarded as

authenticated. All the cell lines were tested negative of mycoplasma contamination by using Mycoalert detection kit (Lonza). The number of passages of cells used in all described experiments are within 20 passages. For androgen stimulation cells were first androgen-starved in phenol-red free RPMI supplement with 5% charcoal-stripped fetal bovine serum for 3 days, then incubated with either ethanol or 1nM R1881 for 24h for gene expression analysis or 10nM R1881 for 16h for chromatin immunoprecipitation. To generate Enz-resistant LNCaP and C4–2B, cells were continuously selected under 1 μM or 10 μM Enz (Selleckchem) respectively for at least 3 months. C4–2B was a kind gift from Dr. Arul Chinnaiyan (University of Michigan). CWR-R1 Enz-resistant cell line was a gift from Dr. Donald Vander Griend (University of Chicago). C4–2B Abiraterone-resistant cell line was a gift from Dr. Allen Gao (University of Califonia Davis). To study MAPK pathway cells were treated with either 1 μM trametinib (MEK1/2 inhibitor) or SCH772984 (ERK1/2 inhibitor) (both Selleckchem) for indicated timepoints. Enz, trametinib, and SCH772984 were dissolved in dimethyl sulfoxide (DMSO) (Sigma). Recombinant human CXCL12 (SDF1) and EGF are purchased from R&D and Sigma-Aldrich correspondingly. Erlotinib is purchased from Selleckchem. All PCR primers used in this study are listed in the Supplementary Table S1. qPCR was performed using SYBR Green by StepOne Plus.

Antibodies, plasmids, and shRNAs

The following antibodies were used: Anti-CXCR7 (GTX100027) (Genetex); Anti-EGFR (A300–387) from Bethyl; Anti-EEA1 (610456) from BD Biosciences; Anti-HDAC1 (ab11966), Anti-H3 (ab1791) and anti-GAPDH (ab9385) from Abcam; Anti-p53 (SC126) and anti-α-tubulin (DM1A) from Santa Cruz; Monoclonal anti-Flag (M2) (F1804) and polyclonal anti-Flag (F7425) from Sigma; Anti-Ki-67 (9027),anti-Phospho-MEK1/2 (Ser217/221) (9154), anti-Phospho-p44/42 MAPK (Erk1/2) (Thr202/Tyr204) (4370), anti-p44/42 MAPK (Erk1/2) (4695), anti-PSA (2475), and anti-ARRB2 (3857) are purchased from Cell Signaling. Anti-CXCR7 (MAB42273) and anti-CXCR4 (MAB170SP) are purchased from R&D systems. pHAGE-Flag-CXCR7 construct was made through subcloning CXCR7 ORF into pHAGE-Flag vector. ARRB2 was first cloned into gateway entry vector pCR8, then transferred into destination vector pLentiSFB with LR clonase (Invitrogen). CXCR7p and CXCR7e guide RNA were subcloned into Lenti-CRISPRV2 vector, CXCR7 shRNAs (TRCN0000014509, TRCN0000363205), ARRB2 (TRCN0000165387, TRCN0000280686) and CXCR4 shRNA (TRCN0000256866) in pLKO vector were purchased from Sigma. Packed lentiviral particles were collected from 293T cultures 48 hours post transfection with lentiviral constructs, pSPAX2 and pMD2G. Viral supernatants were passed through a 0.45-mmfilter, supplemented with 4 ug/mL polybrene, and used to infect prostate cancer cells.

RNA Isolation from patient sample

Briefly, total RNA was isolated from frozen CRPC metastases with RNA STAT-60 (Tel-Test). The purity and yield of the RNA were determined on a NanoDrop by using the sample absorbance at 260 nm and 280 nm, both normalized to the background 340 nm. RNA integrity was assessed on an Agilent 2100 Bioanalyzer, which provided RIN (RNA Integrity Number) values for the samples.

Subcellular protein fractionation and Protein binding assay

To study subcellular protein localization, cells were trypsinized and spun at 500g. Compact cell pellets were lysed in subcellular protein fractionation kit for cultured cells (ThermoFisher) according to product instruction. To determine the interaction between CXCR7 and ARRB2, We performed S-beads protein pull-down as described previously.

Cell proliferation, colony formation and cell invasion assay

Cell proliferation assay was carried out using WST-1 kit according to the manufacturer's instruction (Clontech). To determine synergy of the two drugs, combination index (CI) values were calculated following the manufacturer instruction (CompuSyn). For the colony formation assay, 4×10^3 cells were seeded into 6-well plates and monitored for colony formation for 2 weeks. Then, colonies were stained in 0.25% crystal violet in 20% methanol, photographed, and counted. For cell invasion assay, 2×10^4 cells were plated into the top chamber of matrigel-coated transwell insert (BD Biosciences) in media containing 1%FBS, while 40% FBS condition media, harvested from 3T3, were added to the lower chamber. After 48 hours, the transmigrated cells were stained with 0.25% crystal violet in 20% methanol, imaged and quantified. All assays were triplicated.

Immunofluorescence staining

Cells grown on poly-lysine pre-coated coverslips were fixed in 4% paraformaldehyde in PBS at room temperature for 15 min. After fixation, the cells were permeabilized with a 0.5% Triton X-100 for 15 min and blocked with 3% BSA for 30min. Cells were incubated with anti-Flag (1:2000), anti-EEA1 (1:50) antibodies in blocking buffer at RT for 2 hours, then washed extensively with PBS and incubated with Alexa Fluor–488 or –594 secondary antibodies (Invitrogen) at RT for 1 hour. Nuclei were counterstained with DAPI (Invitrogen) and mounted using Prolong Gold Antifade Reagent (Invitrogen). Images were captured with Axiovert 200 fluorescence microscope (Carl Zeiss) equipped with a Plan Fluor 40× objective lens (1.3 oil) and AxioCam HRc camera. Images were modified by Photoshop CS4 (Adobe).

Immunohistochemistry

Standard immunohistochemistry was performed with antibodies against CXCR7 and p-ERK1/2 on four tissue microarrays representing clinically localized prostate cancer and metastatic prostate cancer using the Bond™ polymer refine detection HRP (Leica Biosystems, DS9800) method. Sections were cut to 4 μm thick, then the sections let be dry in 60°C oven for 1 hour, then the deparaffinization and antigen retrieval (pH6; 20 Minutes) was done on-line using Leica Bond-Max (Leica Biosystems, Buffalo Grove, IL). Antibody was stained as such, the sections washed with bond dewax solution (Leica Biosystems, AR9222) at 72°C then washed with 100% ethanol, followed by washing with bond wash solution, after that sections target antigen were unmasked by incubation in Bond ER 1 Solution (pH6) for 20 min at 100°C (Leica Biosystems, AR9961), subsequently, slides were washed with bond wash solution. Immunostaining for the Primary Antibodies was done by incubation of Primary Antibodies for 15 minutes at room temperature. Following Primary Antibody incubation, sections were incubated with non-conjugated secondary rabbit anti-

mouse IgG for 15 minutes at room temperature. Subsequently, following washing sections were incubated with HRP conjugated polymer anti-rabbit poly-HRP-IgG for 15 minutes at room temperature. Then the endogenous peroxidase activity was blocked with hydrogen peroxide for 5 minutes. Immunoreactivity was visualized with 3, 3-diaminobEnzidine (DAB) Chromogen for 10 minutes at room temperature. Finally, sections were counterstained with Mayer's Hematoxyline for 5 min and Dehydrated by graded alcohol to Xylene using Leica Autostainer XL and mounted by Leica Cover slip (Leica CV5030). Product score of staining percentage and intensity was used as an overall measure. Intensity was scored as negative (score = 0), weak (score = 1), moderate (score = 2), or strong (score = 3) which was multiplied by staining percentage to produce the product score for each core. In total, 30 localized prostate cancer and 106 metastatic prostate cancer tissue cores were evaluable out of 4 tissue microarrays each for CXCR7 and p-ERK1/2 expression.

Fluorescence-activated flow cytometry

Enz^R LNCaP and DMSO LNCaP cell cultures were trypsinized and washed in 1XPBS. Cells were resuspended, and aliquoted in 5×10^5 cells in 100 μl per staining condition. Cell samples were fixed in 0.5x IC Fixation Buffer (eBioscience, Invitrogen) and stained with primary anti-CXCR7 antibodies, clone 11G8 (MAB42273) from R&D, supplemented or not with 1x Permeabilization buffer (eBioscience, Invitrogen). The secondary staining was done with goat anti-rabbit antibodies conjugated with Alexa Fluor-488 antibodies (Invitrogen). Cell nuclei were stained with DAPI (Invitrogen) solution. Sample acquisition was done on BD LSR Fortessa analyser, data were analyzed on FlowJo V10.0.8r1 (FlowJo, LLC).

Chromatin immunoprecipitation (ChIP) and Microarray expression profiling

Briefly, cells were cross-linked with 1% formaldehyde for 10 min and the reaction is quenched by 0.125 M glycine for 5 min at RT. Cells were then rinsed with cold 1xPBS twice, incubated with cell lysis buffer and subsequently nuclear lysis buffer. Chromatin was sonicated and fragmented to a size of 200–500bp, pre-cleared with agarose/protein A or G beads (Upstate), and incubated with 3–5 μg of anti-AR antibodies (N-20) overnight. Protein-DNA complexes were precipitated, washed, and eluted. Microarray expression profiling was performed using HumanHT-12 v 4.0 Expression BeadChip (Illumina). Bead-level data were preprocessed and normalized by GenomeStudio. Differentially expressed genes were identified by Bioconductor limma package (cutoff p<0.005). Heatmap view of differentially expressed genes was created by Cluster and Java Treeview. GO term enrichment was analyzed using DAVID and plot was drawn by R package ggplot2. GSEA analysis was performed according to manufacturer's instruction (Broad institute). The GEO accession number for the data reported in this study is GSE104935.

Tissue Acquisition and Microarray construction

Human PCa specimens were obtained as part of the University of Washington Medical Center PCa Donor Program, which is approved by the University of Washington Institutional Review Board. All specimens for IHC were formalin fixed (decalcified in formic acid for bone specimens), paraffin embedded and examined histologically for the presence of non-necrotic tumor. Tissue microarrays (TMA) were constructed with 1 mm-diameter duplicate cores (number of cores=208) from CRPC patient tissues (number of

patients=34) consisting of visceral metastases and bone metastases (number of sites=104) from patients within 8 hours of death. Tissue microarrays of primary PCa (number of patients=30, number of sites=30) were generated at the Northwestern University Pathology Core through the prostate SPORE program, approved by Northwestern University Institutional Review Board.

Xenograft assay

All procedures were approved by the Northwestern University Institutional Animal Use and Care Committee. Five-week-old male nude athymic BALB/c nu/nu mice (Charles River Laboratory, Wilmington, MA, USA) were purchased for the experiment. To study the function of CXCR7 in Enz resistant PCa growth, 6×10^6 Enz^R C4–2B stably expressing pLKO non-target control or shCXCR7 (1:1 to Matrigel) (BD Biosciences) were inoculated into the right dorsal flank of mice by subcutaneous injection. To evaluate the therapeutic effect of MEKi treatment on Enz-resistant CRPC, 6×10^6 C4–2B cells or Enz^R VCaP were inoculated into the right dorsal flank of mice by subcutaneous injection. Once the tumors reached ~200–300 mm^3, tumor bearing mice were castrated and awaited castration-resistant growth for 2 weeks. Then, mice were randomized into 2 groups: 1) treated with Enz (10 mg/kg/day) alone and 2) Enz (10 mg/kg/day) + trametinib (1 mg/kg/day) for C4–2B or (3mg/kg/day) for VCaP orally for 5 days once a day and total of 4 weeks. Tumor size was measured twice a week and calculated by the formula (length (mm)×width^2(mm^2)×0.5). At the endpoint mice were euthanized and tumor tissues were excised, weighted and extracted for protein lysates.

Results

CXCR7 is upregulated in Enz-resistant PCa

To search for potential drivers of PCa resistance to Enz, we performed expression profiling of DMSO-treated and Enz-resistant (Enz^R) LNCaP cells (Fig. S1A–B). Gene set enrichment analysis (GSEA) demonstrated that AR-induced genes were down-regulated in Enz^R cells, while AR-repressed genes up-regulated, confirming the on-target molecular effects of Enz even in resistant cells (Fig. S1C-D). Analysis of triplicate experiments identified 284 and 294 genes (>2-fold; FDR adjusted p<0.001) that were induced and repressed, respectively, in Enz^R LNCaP cells (Fig. 1A). Gene Ontology (GO) analysis revealed that these genes were involved in previously reported pathways such as steroid hormone biosynthesis but also in novel concepts such as signal peptides and membrane proteins, suggesting increased receptor signaling (Fig. 1B). Interestingly, CXCR7 was among the most upregulated genes in Enz^R cells as compared to the DMSO-treated cells.

To extend this to CRPC models, global expression profiling of Enz^R C4–2B cells (Fig. S1E-F) revealed many up-regulated genes, ranked top among which was CXCR7 (Fig. 1A). QRT-PCR confirmed that CXCR7 was increased by 8 and 5 fold in Enz^R LNCaP and C4–2B cells, respectively (Fig. 1C). Time-course analysis revealed that CXCR7 mRNA began to increase at 3 days after Enz treatment and continued to increase over time (Fig. 1D), while western blotting confirmed CXCR7 protein increase in four Enz^R PCa lines as compared to their DMSO-treated control (Fig. 1E–F), indicating a common mechanism. To determine

whether CXCR7 drives Enz resistance, control and CXCR7-expressing LNCaP cells were treated with increasing doses of Enz (Fig. 1G). Cell growth assays demonstrated that CXCR7 overexpression greatly reduced the sensitivity of LNCaP cells to Enz (Fig. 1G). On the contrary, knockdown of CXCR7 in Enz^R LNCaP cells markedly re-sensitized them to Enz (Fig. 1H), supporting CXCR7 as a driver of PCa Enz resistance.

AR directly inhibits CXCR7 gene transcription

We have recently shown that AR can function as a transcriptional repressor to directly inhibit target genes such as CCN3 (16,17). Interestingly, we found that both CXCR7 mRNA and protein levels were decreased by synthetic androgen R1881 in a dose- and time-dependent manner (Fig. 2A–B & S2A–B). Concordantly, AR knockdown restored CXCR7 expression (Fig. 2C–D). Examining previously published AR ChIP-seq data (18), we found that R1881 treatment which promotes AR nuclear translocation leads to a strong AR binding event at 110kb downstream of the transcription start site (TSS) of the CXCR7 gene and a weaker peak at the promoter (Fig. 2E). ChIP-qPCR confirmed abundant AR occupancy at the CXCR7 enhancer and weaker but significant AR enrichment at the promoter (Fig. 2F). Similar results were also observed in another PCa cell line (Fig. S2C–D).

To examine the importance of the AR binding peaks in regulating CXCR7 expression, we first performed motif analysis and identified a well-centered androgen-response element (ARE) at both CXCR7 promoter and enhancer sites (Fig. S2E–F). Next, we designed guide RNA pairs flanking these ARE elements, which were co-transfected to LNCaP cells with CRISPR-Cas9 lentivirus. CRISPR-Cas9-mediated deletion in a pooled population was validated through PCR analysis of genomic DNA revealing a wildtype and a shorter, ARE-deleted PCR product (Fig. 2G). ChIP-qPCR showed substantially decreased AR recruitment to the CXCR7 enhancer and to a lesser degree the CXCR7 promoter (Fig. 2H). Concordantly, qRT-PCR analysis demonstrated that deletion of the CXCR7 enhancer led to markedly restored expression of CXCR7, while deletion of CXCR7 promoter only slightly increased CXCR7 expression (Fig. 2I). Therefore, the downstream enhancer is essential for CXCR7 repression by AR.

CXCR7 promotes cell survival and invasion in enzalutamide-resistant PCa

To determine the functional roles of CXCR7, we performed CXCR7 knockdown and observed significantly reduced cell proliferation, colony formation, and cell invasion in both Enz^R LNCaP and C4–2B cells, with the amplitude of inhibition proportional to the degree of knockdown (Fig. 3A–D & S3A–D). Next, to examine whether CXCR7 regulates xenograft PCa growth *in vivo*, we inoculated pLKO non-target vector or shCXCR7-transduced Enz^R C4–2B cells subcutaneously into the right dorsal flanks of nude mice. Xenograft tumor growth was measured biweekly. Our data revealed that CXCR7 depletion significantly reduced Enz-resistant PCa tumor growth (Fig. 3E). Accordingly, xenograft tumor weight at the endpoint was also much smaller for the grafts with CXCR7-knockdown cells (Fig. 3F–G).

CXCR7 activates MAPK pathway in enzalutamide-resistant prostate cancer

CXCR7 has been shown to activate the MARK pathway, which is pivotal for cell survival and proliferation (19). Indeed, we observed that pERK1/2 was significantly elevated in Enz^R LNCaP, C4–2B, VCaP and CWR-R1 cells as compared to their DMSO-treated controls (Fig. 4A–B). Further, GSEA demonstrated that a MAPK downstream target gene set, as previously defined (20), was enriched for up-regulation in Enz^R PCa cells (Fig. 4C). To address if this resistance mechanism is specific to enzalutamide or more broadly to androgen inhibition, we also examined the pERK1/2 level in Abiraterone-resistance (Abi^R) cell lines. We demonstrated that CXCR7 is upregulated in Abi^R C4–2B cells with concordance elevation of p-ERK (Fig. S4A). To demonstrate that increased CXCR7 level is responsible for MAPK pathway activation in Enz^R PCa, we silenced CXCR7 in Enz^R LNCaP and observed substantial reduction of pERK1/2 levels, with the amplitude of decrease proportional to the degrees of CXCR7 knockdown (Fig. 4D).

To determine how CXCR7 is activated, we first analyzed CXCL12 expression by ELISA but failed to detect any autocrine production of CXCL12 in Enz^R LNCaP or C4–2B cells. To determine whether exogenous CXCL12 can induce pERK1/2 in Enz^R cells, we serum-starved the cells for 48 hours followed by treatment with 100ng/ml of CXCL12 for up to 5 hours. We found that serum starvation does not affect pERK1/2 levels, suggesting CXCL12-independent, constitutive activation of CXCL12 (Fig. 4E). Exogenous CXCL12 further increased pERK1/2 levels after 2 hours of treatment, a delayed response typical of CXCR7-mediated signaling (21). Interestingly, exogenous CXCL12 also induced pERK1/2 in the control cells, although to a lesser degree, likely due to less amount of CXCR7 in these cells. Recent studies have suggested that EGF-stimulated EGFR, which results in EGFR phosphorylation (pEGFR) and activation, may interact with CXCR7 and stimulate pERK1/2 (13,14). However, our data showed that EGFR expression was abolished to an undetectable level, rather than increased, in Enz^R cells as compared to control and pEGFR could not be detected, precluding its role in this context (Fig. S4B-C).

We next attempted to examine whether CXCR4 is required for CXCR7 activation in PCa. Firstly, we found that CXCR4 was expressed at low levels in most PCa lines; CXCR7 level was several magnitudes higher (Fig. 4F). As controls, CXCR4 level was high in 293T cells, wherein CXCR7 was not expressed. In expression profiling data, we did not observe CXCR4 up-regulation in Enz-resistant PCa cells. Moreover, CXCR4 knockdown in Enz^R cells (Fig. S4D) did not affect pERK1/2 level, while CXCR7 knockdown abolished pERK1/2 (Fig. 4G). In aggregate, we demonstrate that MAPK pathway in Enz^R PCa cells is activated by CXCR7 in a CXCR4- and CXCL12-independent manner but may be further enhanced by CXCL12, if present.

CXCR7 activates MAPK pathway through the recruitment of β-Arrestin 2

CXCR7 is known as a membrane protein that, when activated, internalizes into the endosomes forming a complex with ARRB2, which acts as a scaffold protein for MAPK protein assembly and activation (10). We performed flow cytometry on non-permeabilized PCa cells and indeed found that CXCR7 was present on the plasma membrane of LNCaP and C4–2B cells and was further increased in their Enz-resistant derivatives (**Fig. 5A &**

S5A). Further, fractionation of protein lysates from Enz[R] LNCaP cells showed CXCR7 localization exclusively to the membranous fraction, which contains membranes of both plasma and cytoplasmic organelle (e.g. endosome) (Fig. 5B). We noted that pERK1/2 was present primarily in cytoplasmic and membrane fractions but very weak in nuclear fractions, supporting its activation by CXCR7-ARRB2 complex. Moreover, immunofluorescent co-staining validated that CXCR7 localized mainly in cytoplasmic aggregates, co-localizing with early endosome marker EEA1 and ARRB2 (Fig. 5C–D). Lastly, co-immunoprecipitation showed that anti-Flag pull down of flag-ARRB2 expressed in Enz[R] LNCaP cells indeed enriched CXCR7, supporting CXCR7-ARRB2 interaction (Fig. 5E).

To examine if ARRB2 is involved in CXCR7-mediated MAPK activation in Enz-resistant PCa cells, we knocked down ARRB2 and evaluated pERK1/2 by western blotting. Depletion of ARRB2 markedly attenuated ERK1/2 phosphorylation (Fig. 5F), echoing the decrease of pERK1/2 upon CXCR7 depletion. Moreover, in a rescue experiment ARRB2 knockdown abolished pERK1/2 that were induced by ectopic CXCR7 in LNCaP cells, supporting that ARRB2 is required for CXCR7-mediated activation of MAPK (Fig. 5G). Furthermore, analogous to CXCR7 depletion (Fig. 3), ARRB2 knockdown in Enz-resistant cells led to remarkable reduction in cell proliferation, colony formation, and cell invasion (Fig. 5H–J & S5B). We thus conclude that CXCR7 activates MAPK pathway in Enz-resistant cells through cytoplasmic internalization and the recruitment of ARRB2.

CXCR7 expression and MAPK signaling are elevated in metastatic CRPC

To determine the clinical relevance of the CXCR7-MAPK pathway, we analyzed public microarray dataset and observed significant CXCR7 up-regulation in CRPC relative to localized PCa in (22,23) (Fig. 6A & S6A). Further, analysis of RNA-seq data (24) showed substantial CXCR7 up-regulation in CRPC compared to primary PCa (Fig. 6B). Further, qRT-PCR of tissue samples confirmed that CXCR7 mRNA level was increased in CRPC relative to localized PCa and was further increased post-abiraterone and/or Enz treatment (Fig. 6C). Moreover, re-analysis of 122 CRPC transcriptomes generated by the International Stand Up To Cancer/Prostate Cancer Foundation (SU2C/PCF) Prostate Cancer Dream Team (25) showed a strong ($p=4\times10^{-11}$) correlation of CXCR7 expression and a MEK-functional-activation signature (26) (Fig. S6B).

Next, we performed immunohistochemical (IHC) assays on several tissue microarrays (TMA) containing localized or metastatic PCa. We found that CXCR7 staining was very high in endothelial cells, which was consistent with previous reports (27), supporting the specificity of the assay. CXCR7 was almost undetectable in localized PCa but expressed strongly in about 30% of CRPC (Fig. 6D–E). Concordantly, pERK1/2 staining was weak in localized PCa and was strongly increased in CRPC (Fig. 6F–G). Importantly, we analyzed a single CRPC available worldwide, that progressed on Enz and was subsequently treated with MEK inhibitor trametinib (Tra). After two years on Tra with an ongoing radiographic response characterized by an objective reduction in the size of enlarged retroperitoneal lymph nodes, the patient died of an unrelated cause. Lymph node metastases were collected post-Enz but prior to Tra. IHC staining revealed indeed a concordant increase of CXCR7 and pERK staining compared to localized PCa (Fig. 6H). Taken together, our data confirmed

CXCR7 and MAPK pathway up-regulation in CRPC and suggested them as promising targets for therapeutic intervention.

Trametinib inhibits enzalutamide-resistant PCa growth *in vitro* and *in vivo*

To test the effects of MAPK inhibitors, western blot analysis showed that Tra at 2μM is sufficient to abolish pERK1/2 in LNCaP cells induced by Enz (0.5μM) (Fig. 7A). The specificity of Tra on ERK signaling was validated as various known CXCR7 downstream phospho-proteins such as pAKT, pSTAT3, pJNK, pMEK1/2, and p-p38 remained unaffected upon Tra treatment (Fig. S7A). Concordantly, cell growth assay and colony formation assays showed combinatorial effects of Enz and Tra in inhibiting proliferation of LNCaP and VCaP cells (Fig. 7B–C & S7B–C). In addition, we evaluated the combination effect of Enz and Tra with the use of Compusyn software. Combination index (CI) revealed that all the tested doses of Enz+Tra exhibit synergistic interaction (CI<1) (Fig. 7D & S7D).

Next, to test the therapeutic effects of Tra *in vivo*, Enz^R VCaP or Enz^R C4–2B cells were inoculated subcutaneously into the dorsal flanks of nude mice. Upon initial tumor formation, all mice were castrated. Once tumors stabilized after castration, mice were treated with either Enz alone or in combination with Tra. Tumor size were measured twice per week. Enz^R xenografts treated with Enz alone progressed steadily as expected. Significantly, xenografts treated with the drug combination not only failed to progress but showed remarkable tumor regression (Fig. 7E–F & S7E-F). Accordingly, average tumor weight from mice received combinatorial treatment was significantly lower than those received Enz monotherapy (Fig. 7G & S7G). Western blotting confirmed decreased pERK1/2 by Tra (Fig. 7H & S7H). Thus, our data strongly suggest that the MEK inhibitor Tra may be useful for the treatment of Enz-resistant CRPC.

Discussion

Recent studies have reported AR as a transcriptional repressor, which is orchestrated by other transcriptional repressors such as EZH2 and LSD1 (16,28). Here, we identify CXCR7 as a direct target of AR-mediated transcription repression. In contrast to a recent paper reporting AR regulation of CXCR7 through the promoter (14), we used ChIP and CRISPR-Cas9 system to establish that CXCR7 is repressed primarily by AR-bound enhancer 110kb away from the TSS. AR binding at the CXCR7 promoter is much weaker and is most likely indirect, due to the AR-bound enhancer forming chromatin loops to the promoter, which is typical for AR-regulated genes (17,29,30). Similar to CXCR7, AR-repressed genes such as c-MET, HOTAIR, and SOX2 have previously been shown up-regulated upon ADT and act as oncogenes to drive CRPC (30–32).

Since its initial discovery as a cognate receptor of CXCL12 in 2006 (33), CXCR7 has been reported to act through both constitutive and ligand-dependent manner (11,19,34,35). Concordantly, we found that elevated CXCR7 in Enz-resistant PCa turns on downstream signaling independently of CXCL12, albeit the effect can be further enhanced by CXCL12 stimulation. Although a previous study have suggested the forming of CXCR4-CXCR7 heterodimer upon ectopic expression (36), endogenous complex has not been isolated. Our data showed that CXCR4 is barely expressed in PCa cell lines, wherein CXCR7 was

expressed at a level of several magnitudes higher. Further, only CXCR7, but not CXCL12 and CXCR4, was up-regulated in Enz-resistant lines and our data showed that CXCR4 is not required for CXCR7-stimulated MAPK activation. We also tested if CXCR7 becomes constitutively active due to emergence of gene mutation, but no mutation in *CXCR7* were detected in our resistance lines, which suggested that CXCR7 activation is less likely due to acquired mutation. A recent study of obese HiMyc mice revealed high levels of CXCL12 in prostate stroma and high staining of CXCR4 and CXCR7 proteins in the epithelial compartment of mice tumors (37). It would be interesting to examine CXCR7 signaling within the tumor microenvironment, which however is beyond the scope of the present study.

Unlike CXCR4, activated CXCR7 interacts with ARRB2, rather than G proteins, to stimulate receptor internalization and downstream MAPK/ERK activation (10). Indeed, we found that ARRB2 is required for the roles of CXCR7 in activating MAPK/ERK signaling and promoting Enz-resistant PCa. This is in contrast to a recent study reporting a role of ARRB2 in suppressing CXCR7-mediated EGFR transactivation upon exogenous EGF stimulation (38). We propose that this is due to promiscuous CXCR7 interaction with abundant EGF that was exogenously provided, which may compete with ARRB2. However, whether this interaction is relevant in a physiological setting is unclear.

Our data suggests CXCR7 and MAPK/ERK pathway as promising targets for therapeutic intervention. Many attempts have been made to generate CXCR7 antagonists with CCX771 being the most prominent. However, recent studies have unfortunately determined that CCX771, despite its ability to bind CXCL12, actually acts as an agonist (39), which raises concerns regarding studies using CCX771 as CXCR7 antagonist (40) . Here, we took advantage of the readily available MAPK inhibitors to block CXCR7 downstream pathways. We are aware that MAPK targeting as a single agent may lead to rapid development of resistance (41) and was suggested to be used in combination with other targeted agents to mitigate drug resistance (42). Our data strongly support that Tra in combination with Enz may be highly effective in the treatment of CRPC.

Supplementary Material

Refer to Web version on PubMed Central for supplementary material.

Acknowledgements

References

1. Yuan X, Balk SP. Mechanisms mediating androgen receptor reactivation after castration. Urol Oncol 2009;27:36–41 [PubMed: 19111796]

2. Chen CD, Welsbie DS, Tran C, Baek SH, Chen R, Vessella R, et al. Molecular determinants of resistance to antiandrogen therapy. Nat Med 2004;10:33–9 [PubMed: 14702632]

3. Scher HI, Fizazi K, Saad F, Taplin ME, Sternberg CN, Miller K, et al. Increased survival with enzalutamide in prostate cancer after chemotherapy. N Engl J Med 2012;367:1187–97 [PubMed: 22894553]

4. Claessens F, Helsen C, Prekovic S, Van den Broeck T, Spans L, Van Poppel H, et al. Emerging mechanisms of enzalutamide resistance in prostate cancer. Nat Rev Urol 2014;11:712–6 [PubMed: 25224448]

5. Joseph JD, Lu N, Qian J, Sensintaffar J, Shao G, Brigham D, et al. A clinically relevant androgen receptor mutation confers resistance to second-generation antiandrogens enzalutamide and ARN-509. Cancer discovery 2013;3:1020–9 [PubMed: 23779130]

6. Korpal M, Korn JM, Gao X, Rakiec DP, Ruddy DA, Doshi S, et al. An F876L mutation in androgen receptor confers genetic and phenotypic resistance to MDV3100 (enzalutamide). Cancer discovery 2013;3:1030–43 [PubMed: 23842682]

7. Antonarakis ES, Lu C, Wang H, Luber B, Nakazawa M, Roeser JC, et al. AR-V7 and resistance to enzalutamide and abiraterone in prostate cancer. N Engl J Med 2014;371:1028–38 [PubMed: 25184630]

8. Arora VK, Schenkein E, Murali R, Subudhi SK, Wongvipat J, Balbas MD, et al. Glucocorticoid receptor confers resistance to antiandrogens by bypassing androgen receptor blockade. Cell 2013;155:1309–22 [PubMed: 24315100]

9. Mu P, Zhang Z, Benelli M, Karthaus WR, Hoover E, Chen CC, et al. SOX2 promotes lineage plasticity and antiandrogen resistance in TP53- and RB1-deficient prostate cancer. Science 2017;355:84–8 [PubMed: 28059768]

10. Lefkowitz RJ, Shenoy SK. Transduction of receptor signals by beta-arrestins. Science 2005;308:512–7 [PubMed: 15845844]

11. Luker KE, Steele JM, Mihalko LA, Ray P, Luker GD. Constitutive and chemokine-dependent internalization and recycling of CXCR7 in breast cancer cells to degrade chemokine ligands. Oncogene 2010;29:4599–610 [PubMed: 20531309]

12. Wang J, Shiozawa Y, Wang J, Wang Y, Jung Y, Pienta KJ, et al. The role of CXCR7/RDC1 as a chemokine receptor for CXCL12/SDF-1 in prostate cancer. The Journal of biological chemistry 2008;283:4283–94 [PubMed: 18057003]

13. Singh RK, Lokeshwar BL. The IL-8-regulated chemokine receptor CXCR7 stimulates EGFR signaling to promote prostate cancer growth. Cancer Res 2011;71:3268–77 [PubMed: 21398406]

14. Hoy JJ, Kallifatidis G, Smith DK, Lokeshwar BL. Inhibition of androgen receptor promotes CXC-chemokine receptor 7-mediated prostate cancer cell survival. Sci Rep 2017;7:3058 [PubMed: 28596572]

15. Saha A, Ahn S, Blando J, Su F, Kolonin MG, DiGiovanni J. Proinflammatory CXCL12-CXCR4/CXCR7 signaling axis drives Myc-induced prostate cancer in obese mice. Cancer Res 2017

16. Zhao JC, Yu J, Runkle C, Wu L, Hu M, Wu D, et al. Cooperation between Polycomb and androgen receptor during oncogenic transformation. Genome Res 2012;22:322–31 [PubMed: 22179855]

17. Wu L, Runkle C, Jin HJ, Yu J, Li J, Yang X, et al. CCN3/NOV gene expression in human prostate cancer is directly suppressed by the androgen receptor. Oncogene 2014;33:504–13 [PubMed: 23318417]

18. Yu J, Yu J, Mani RS, Cao Q, Brenner CJ, Cao X, et al. An integrated network of androgen receptor, polycomb, and TMPRSS2-ERG gene fusions in prostate cancer progression. Cancer Cell 2010;17:443–54 [PubMed: 20478527]

19. Rajagopal S, Kim J, Ahn S, Craig S, Lam CM, Gerard NP, et al. beta-arrestin- but not G protein-mediated signaling by the "decoy" receptor CXCR7. P Natl Acad Sci USA 2010;107:628–32

20. Pratilas CA, Taylor BS, Ye Q, Viale A, Sander C, Solit DB, et al. (V600E)BRAF is associated with disabled feedback inhibition of RAF-MEK signaling and elevated transcriptional output of the pathway. Proc Natl Acad Sci U S A 2009;106:4519–24 [PubMed: 19251651]

21. McGinn OJ, Marinov G, Sawan S, Stern PL. CXCL12 receptor preference, signal transduction, biological response and the expression of 5T4 oncofoetal glycoprotein. J Cell Sci 2012;125:5467–78 [PubMed: 22956548]

22. Yu YP, Landsittel D, Jing L, Nelson J, Ren B, Liu L, et al. Gene expression alterations in prostate cancer predicting tumor aggression and preceding development of malignancy. J Clin Oncol 2004;22:2790–9 [PubMed: 15254046]

23. Cai C, Wang H, He HH, Chen S, He L, Ma F, et al. ERG induces androgen receptor-mediated regulation of SOX9 in prostate cancer. J Clin Invest 2013;123:1109–22 [PubMed: 23426182]

24. Iyer MK, Niknafs YS, Malik R, Singhal U, Sahu A, Hosono Y, et al. The landscape of long noncoding RNAs in the human transcriptome. Nat Genet 2015;47:199–208 [PubMed: 25599403]

25. Robinson D, Van Allen EM, Wu YM, Schultz N, Lonigro RJ, Mosquera JM, et al. Integrative Clinical Genomics of Advanced Prostate Cancer. Cell 2015;162:454 [PubMed: 28843286]

26. Dry JR, Pavey S, Pratilas CA, Harbron C, Runswick S, Hodgson D, et al. Transcriptional pathway signatures predict MEK addiction and response to selumetinib (AZD6244). Cancer Res 2010;70:2264–73 [PubMed: 20215513]

27. Berahovich RD, Zabel BA, Lewen S, Walters MJ, Ebsworth K, Wang Y, et al. Endothelial expression of CXCR7 and the regulation of systemic CXCL12 levels. Immunology 2014;141:111–22 [PubMed: 24116850]

28. Cai C, He HH, Chen S, Coleman I, Wang H, Fang Z, et al. Androgen receptor gene expression in prostate cancer is directly suppressed by the androgen receptor through recruitment of lysine-specific demethylase 1. Cancer Cell 2011;20:457–71 [PubMed: 22014572]

29. Wang Q, Li W, Liu XS, Carroll JS, Janne OA, Keeton EK, et al. A hierarchical network of transcription factors governs androgen receptor-dependent prostate cancer growth. Molecular cell 2007;27:380–92 [PubMed: 17679089]

30. Zhang A, Zhao JC, Kim J, Fong KW, Yang YA, Chakravarti D, et al. LncRNA HOTAIR Enhances the Androgen-Receptor-Mediated Transcriptional Program and Drives Castration-Resistant Prostate Cancer. Cell Rep 2015;13:209–21 [PubMed: 26411689]

31. Verras M, Lee J, Xue H, Li TH, Wang Y, Sun Z. The androgen receptor negatively regulates the expression of c-Met: implications for a novel mechanism of prostate cancer progression. Cancer Res 2007;67:967–75 [PubMed: 17283128]

32. Kregel S, Kiriluk KJ, Rosen AM, Cai Y, Reyes EE, Otto KB, et al. Sox2 is an androgen receptor-repressed gene that promotes castration-resistant prostate cancer. PLoS One 2013;8:e53701 [PubMed: 23326489]

33. Burns JM, Summers BC, Wang Y, Melikian A, Berahovich R, Miao Z, et al. A novel chemokine receptor for SDF-1 and I-TAC involved in cell survival, cell adhesion, and tumor development. The Journal of experimental medicine 2006;203:2201–13 [PubMed: 16940167]

34. Ray P, Mihalko LA, Coggins NL, Moudgil P, Ehrlich A, Luker KE, et al. Carboxy-terminus of CXCR7 regulates receptor localization and function. Int J Biochem Cell Biol 2012;44:669–78 [PubMed: 22300987]

35. Lin L, Han MM, Wang F, Xu LL, Yu HX, Yang PY. CXCR7 stimulates MAPK signaling to regulate hepatocellular carcinoma progression. Cell Death Dis 2014;5:e1488 [PubMed: 25341042]

36. Levoye A, Balabanian K, Baleux F, Bachelerie F, Lagane B. CXCR7 heterodimerizes with CXCR4 and regulates CXCL12-mediated G protein signaling. Blood 2009;113:6085–93 [PubMed: 19380869]

37. Saha A, Ahn S, Blando J, Su F, Kolonin MG, DiGiovanni J. Proinflammatory CXCL12-CXCR4/CXCR7 Signaling Axis Drives Myc-Induced Prostate Cancer in Obese Mice. Cancer Res 2017;77:5158–68 [PubMed: 28687617]

38. Kallifatidis G, Munoz D, Singh RK, Salazar N, Hoy JJ, Lokeshwar BL. beta-Arrestin-2 Counters CXCR7-Mediated EGFR Transactivation and Proliferation. Mol Cancer Res 2016;14:493–503 [PubMed: 26921391]

39. Zabel BA, Wang Y, Lewen S, Berahovich RD, Penfold ME, Zhang P, et al. Elucidation of CXCR7-mediated signaling events and inhibition of CXCR4-mediated tumor cell transendothelial migration by CXCR7 ligands. J Immunol 2009;183:3204–11 [PubMed: 19641136]

40. Luo Y, Azad AK, Karanika S, Basourakos SP, Zuo X, Wang J, et al. Enzalutamide and CXCR7 inhibitor combination treatment suppresses cell growth and angiogenic signaling in castration-resistant prostate cancer models. Int J Cancer 2018;142:2163–74 [PubMed: 29277895]

41. Davies MA, Kopetz S. Overcoming resistance to MAPK pathway inhibitors. J Natl Cancer Inst 2013;105:9–10 [PubMed: 23250957]

42. Brechbiel J, Miller-Moslin K, Adjei AA. Crosstalk between hedgehog and other signaling pathways as a basis for combination therapies in cancer. Cancer treatment reviews 2014;40:750–9 [PubMed: 24613036]

The statement of Significance

Findings identify CXCR7-mediated MAPK activation as a mechanism of resistance to second generation anti-androgen therapy, highlighting the therapeutic potential of MAPK/ERK inhibitors in castration-resistant prostate cancer.
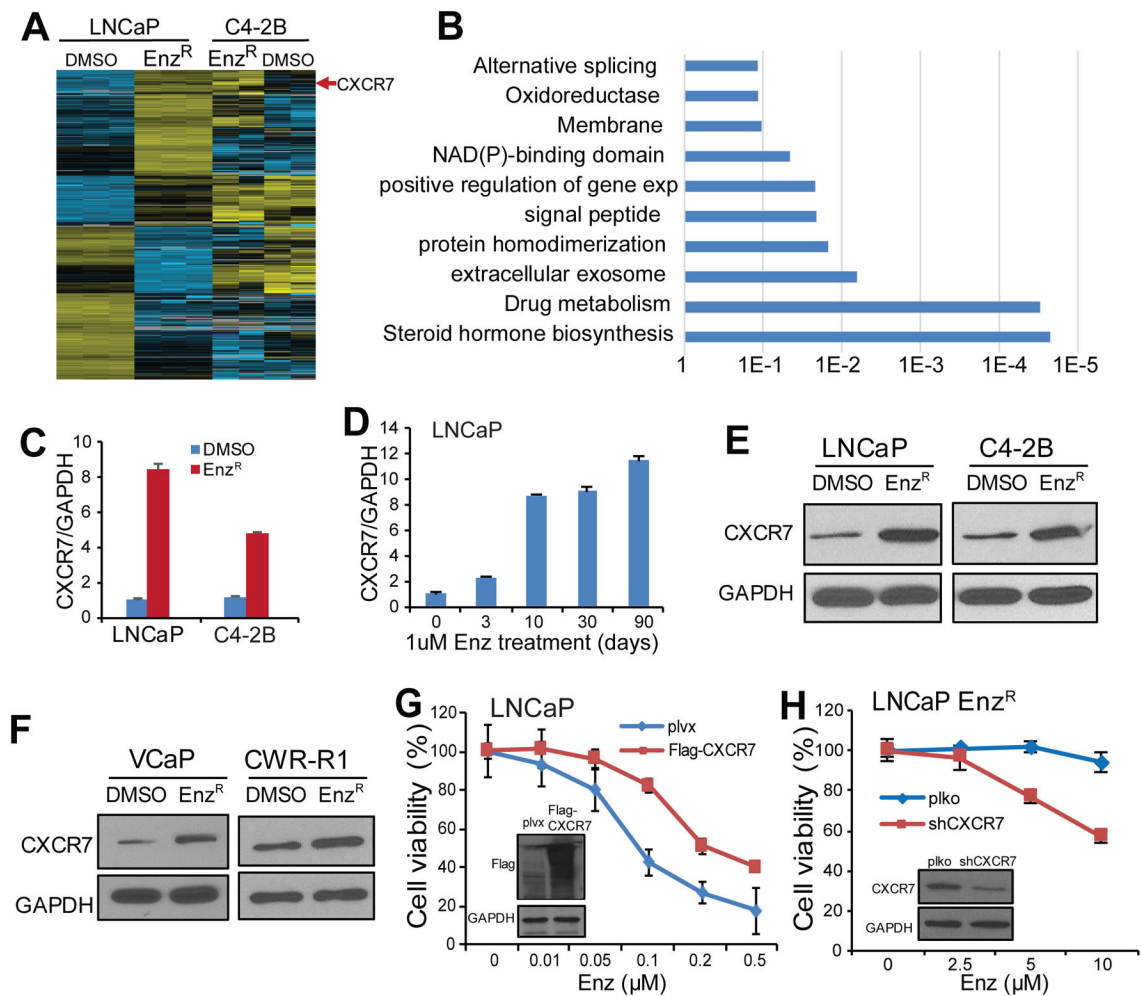
Figure 1. CXCR7 is upregulated in Enz-resistant prostate cancer
A. Heatmap view of differentially expressed genes in Enz-resistant cells. LNCaP and C4–2B cells were treated respectively with 1μM and 10μM of Enz (Enz[R]) or DMSO vehicle control for months to develop resistant lines. Cells were then collected for microarray profiling of gene expression. Arrow depicts the position of CXCR7.

B. GO categories that are enriched by gene sets differentially expressed in Enz[R] versus control cells (**A**). X-axis: GO-enrichment *p* values.

C. CXCR7 is upregulated in Enz-resistant cells. qRT-PCR analysis of CXCR7 mRNA level in Enz[R] LNCaP or C4–2B compared to their respective control cells. Data were normalized to GAPDH. Data shown are mean ± SEM.

D. Time-dependent up-regulation of CXCR7 by Enz. LNCaP cells were treated with 1μM MDV3100 over a time course, and CXCR7 mRNA was analyzed by qRT-PCR. Data were normalized to GAPDH. Data shown are mean ± SEM.

E-F. Western blot analysis of CXCR7 protein levels in a panel of Enz[R] LNCaP, C4–2B, VCaP, and CWR-R1 cells compared to their respective DMSO-treated cells.

G-H. CXCR7 overexpression confers resistance to Enz. LNCaP cells with either empty vector or Flag-CXCR7 overexpressing (**G**) or Enz[R] LNCaP cells infected with shCtrl or shCXCR7 (**H**) were treated with titrated doses of Enz for 5 days. Cell viability was
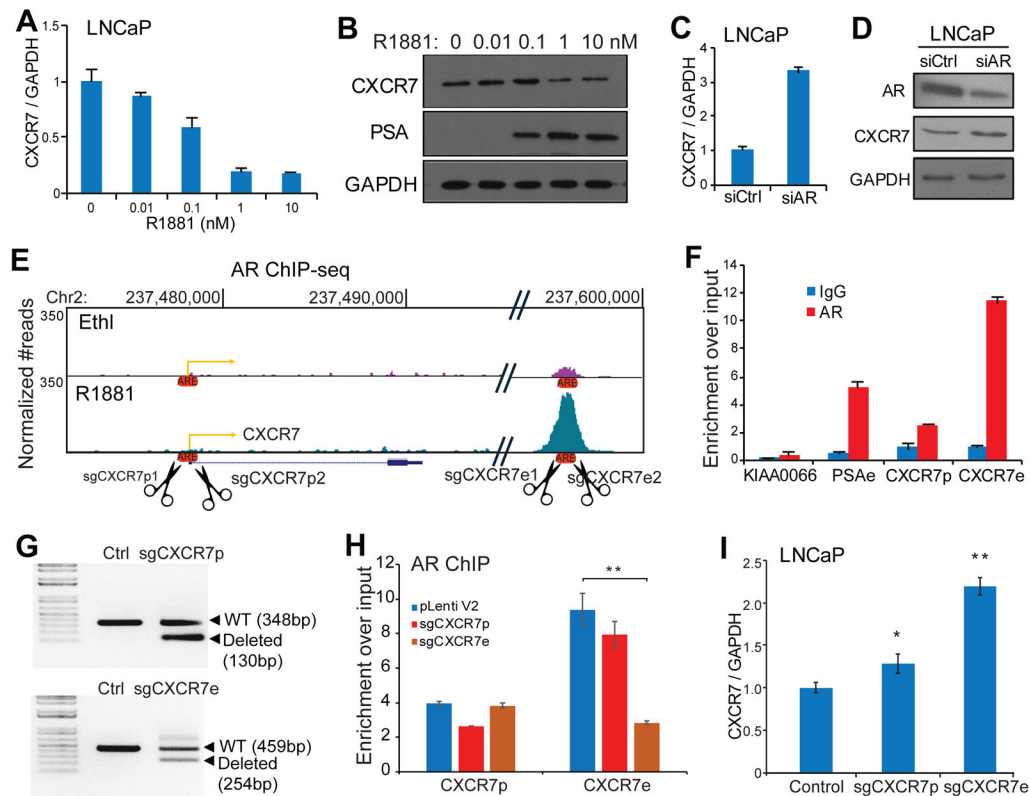
quantitated by WST-1 assay. Data shown are mean (±SEM). Inset: western blotting confirm gene overexpression or knockdown.

Figure 2. AR directly represses CXCR7 gene transcription.

A-B. Androgen represses CXCR7 expression. LNCaP cells were treated with different concentrations of R1881 (synthetic androgen) and then harvested for qRT-PCR (**A**) and western blotting (**B**) analysis.

C-D. AR depletion restores CXCR7 expression. LNCaP cells were subjected to control (siCtrl) and AR-targeted siRNA and then harvested for qRT-PCR (**C**) and western blot (**D**) analysis.

E. AR directly occupies the CXCR7 promoter and enhancer. Previous AR ChIP-seq in hormone-starved LNCaP cells treated with ethanol (EthI) or R1881 was re-analyzed and ChIP-seq signal around CXCR7 gene is shown.

F. AR and IgG ChIP were performed in LNCaP cells and ChIP-qPCR was carried out using primers flanking the CXCR7 promoter or enhancer regions. Data shown are mean (±SEM).

G-I. Deletion of ARE sites at CXCR7 promoter or enhancer impairs AR recruitment and CXCR7 expression. LNCaP cells were infected with Cas9-containing pLENTI.V2 control, sgCXCR7p1 and p2, and sgCXCR7e1 and e2 for 48 hours. Pooled population were analyzed by genomic DNA PCR for CRISPR-Cas9-mediated deletion leading to a wildtype and a deleted mutant band (**G**). AR ChIP was performed in these cells followed by qPCR analysis of AR occupancy on the CXCR7 promoter (CXCR7p) and enhancer (CXCR7e) (**H**). CXCR7 expression in these cells were determined by qRT-PCR analysis (**I**). Data shown are mean (±SEM). *p<0.05; ** p<0.01.
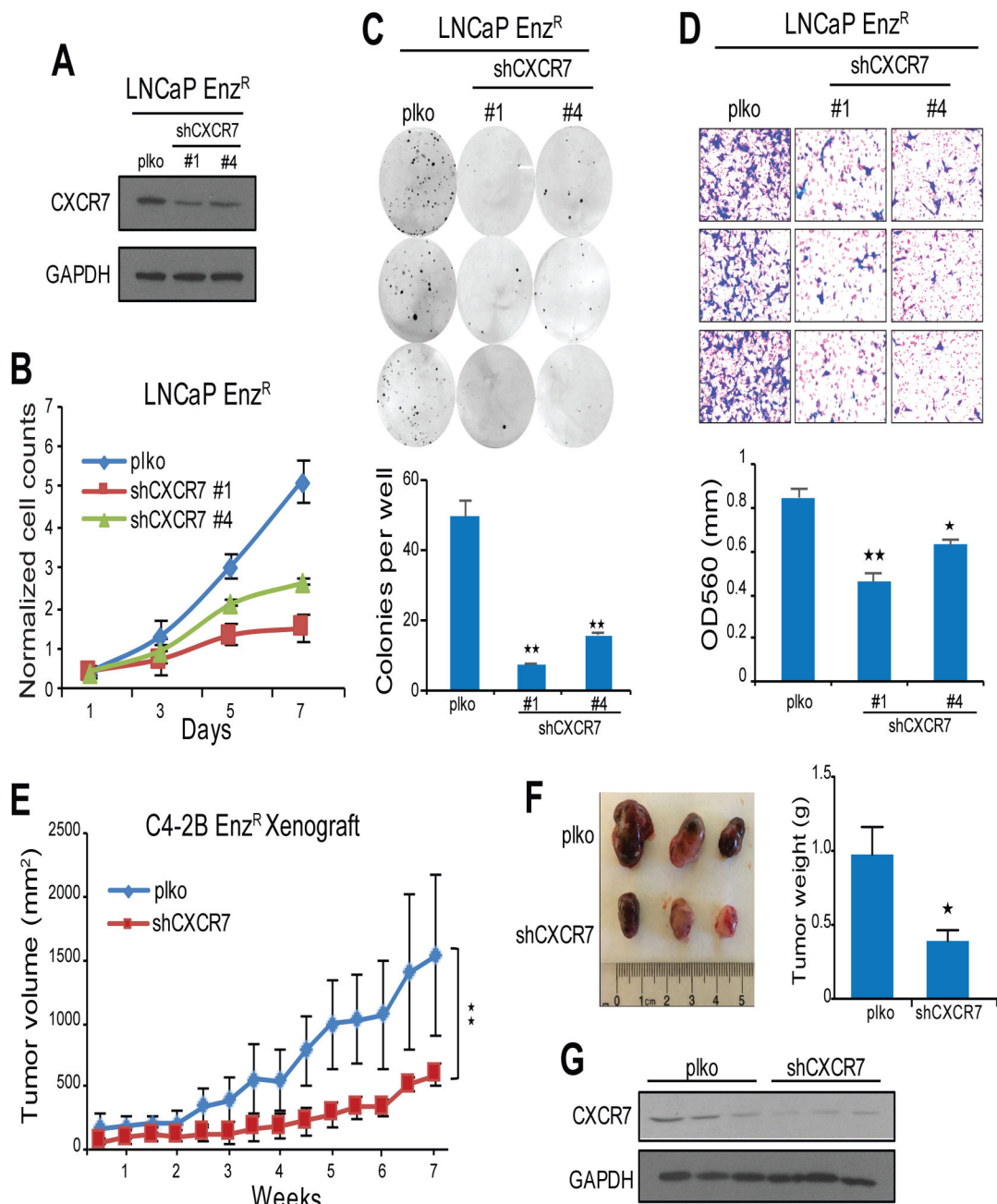
Figure 3. CXCR7 expression drives Enz-resistant prostate cancer cell growth and invasion *in vitro* and xenograft tumor growth *in vivo*.

A. shRNA-mediated knockdown of CXCR7. LNCaP cells were infected with two different shRNAs targeting CXCR7 for 48hrs and then subjected to western blotting.

B-D. CXCR7 drives Enz-resistant cell growth and invasion. Enz[R] LNCaP cells infected with shCtrl, shCXCR7–1 or shCXCR7–2 were subjected to WST1 cell proliferation assay **(B),** colony formation assay **(C),** and Boyden chamber invasion assay **(D)**.

E-G. Knockdown of CXCR7 reduces xenograft PCa tumor growth. Control and CXCR7-knockdown Enz[R] C4–2B cells were injected subcutaneously into the right dorsal flanks of
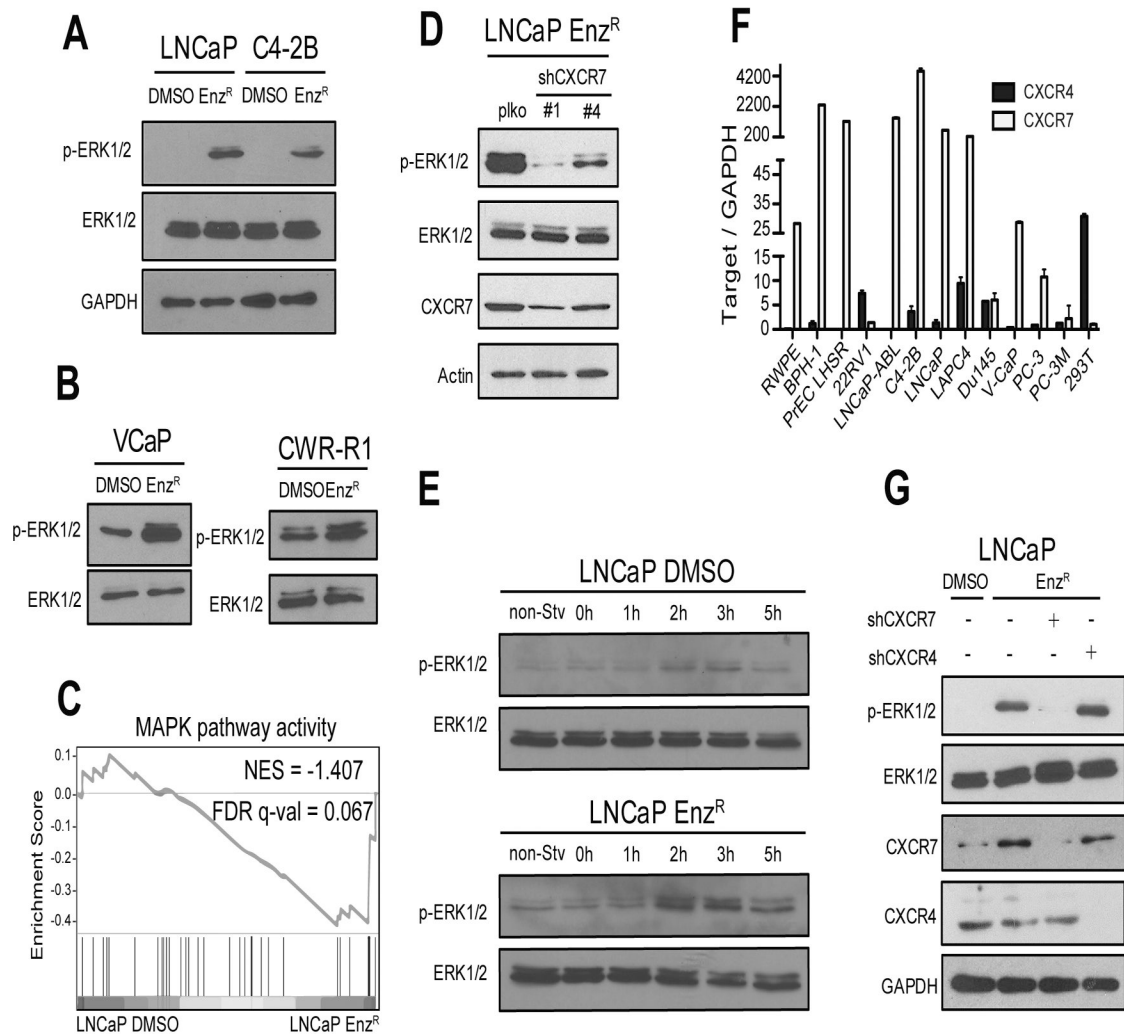
nude mice. Tumor size was measured twice per week and compared between groups by ANOVA (**p<0.01) **(E)**. Tumors excised from euthanized mice were weighted, photographed, and compared (T test, *p<0.05). **(F)**. CXCR7 knockdown in tumors was confirmed by western blotting (**G**).

Figure 4. Elevated CXCR7 in Enz^R PCa cells activates MAPK pathway independently of CXCR4 and CXCL12.

A-B. MAPK/ERK pathway was activated in Enz-resistant cells. Protein lysates of indicated cell lines were subjected to western blot analyses using pERK1/2 and total ERK1/2 antibodies, respectively. GAPDH was used as a loading control.

C. MARK pathway is activated in Enz^R LNCaP. GSEA analysis was performed to determine the enrichment of MARK downstream target gene set in gene expression dataset profiling DMSO LNCaP and Enz^R LNCaP.

D. Knockdown of CXCR7 suppresses MAPK/ERK pathway. Protein lysates from Enz^R LNCaP treated with shCtrl or two different shCXCR7 were analyzed by immunoblotting. Actin was used as a loading control.

E. CXCR7 activates MAPK/ERK through ligand-dependent and –independent mechanisms. Control and Enz^R LNCaP cells were serum-starved for 48 hours and then stimulated with CXCL12 (100ng/ml) for up to 5 hours. Cell lysates were collected at indicated time-points and subjected for immunoblotting.

F. CXCR4 is expressed at low levels in PCa cell lines. QRT-PCR was performed in in a panel of PCa cell lines and 293T using gene-specific primers.
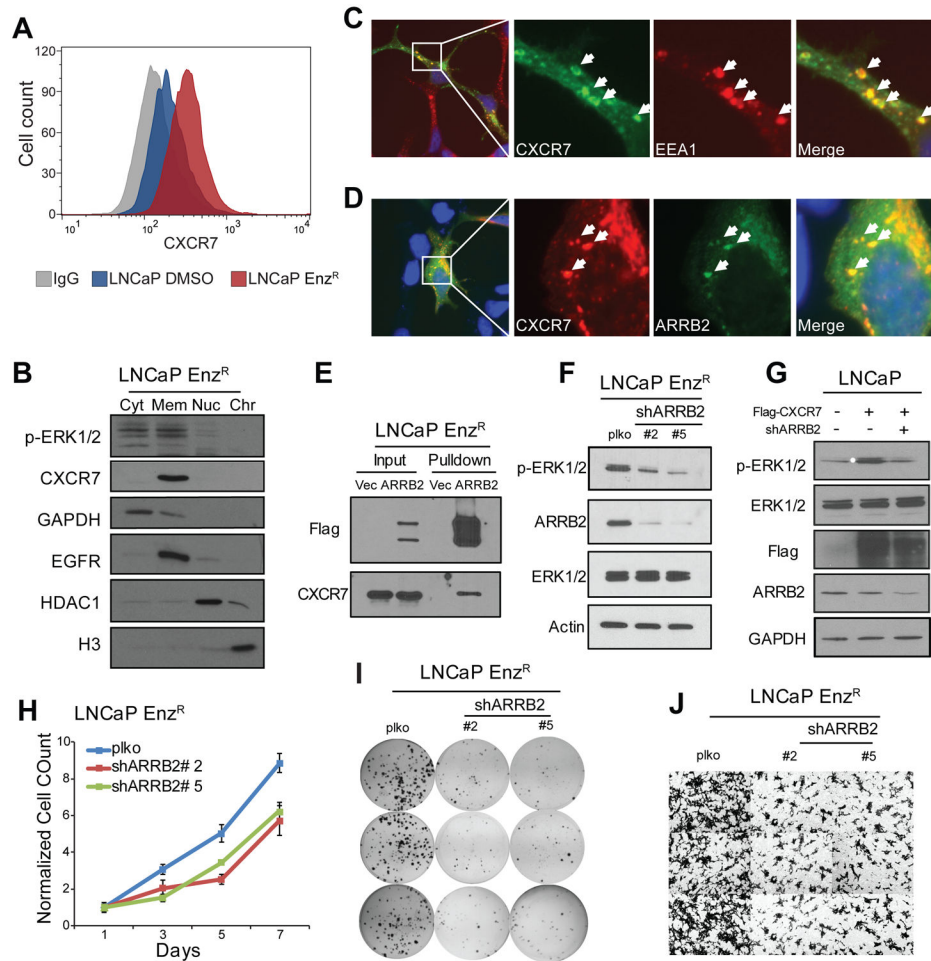
G. CXCR4 is dispensable for CXCR7-medated MARK pathway activation. Protein lysates from DMSO LNCaP or Enz[R] LNCaP cells treated with shCtrl, shCXCR4 or shCXCR7 were analyzed by immunoblotting **(G)**.

Figure 5. CXCR7 activates MAPK pathway through β-Arrestin 2.
A. CXCR7 localizes to plasma membrane. DMSO LNCaP and Enz^R LNCaP cells were stained by IgG or anti-CXCR7 antibodies and subjected to FACS analysis.
**B.** CXCR7 co-fractionates with pERK1/2. Subcellular protein fractionation was performed using Enz^R LNCaP. Protein samples from cytoplasmic (Cyto), membranous (Mem), nucleoplasmic (Nuc) and chromatin (Chr) fractions were subjected to immunoblotting using indicated antibodies.
C-D. CXCR7 co-localizes with ARRB2 to the endosomes. LNCaP cells transiently expressing Flag-CXCR7 **(C)** or Flag-CXCR7 + HA-ARRB2 **(D)** were fixed and subjected to immunostaining using indicated antibodies.
E. CXCR7 forms a complex with ARRB2 in Enz^R LNCaP cells. S-beads pull down was performed using protein lysate of Enz^R LNCaP expressing empty vector or lenti-SFB ARRB2. The precipitated protein was analyzed by immunoblot using indicated antibodies.
F-G. CXCR7 activation of MAPK pathway was attenuated by knockdown of ARRB2. Protein lysates from Enz^R LNCaP treated with shCtrl or two different shRNAs against ARRB2 were analyzed by immunoblot using indicated antibodies. Actin was used as a loading control **(F)**. Protein lysates from LNCaP overexpressing empty vector, Flag-CXCR7 or Flag-CXCR7 + shARRB2 were analyzed by immunoblot using indicated antibodies **(G)**.

H-I. Knockdown of ARRB2 inhibits Enz^R LNCaP cell growth. shCtrl or shARRB2 infected Enz^R LNCaP were plated for WST-1 cell growth assay **(H)** and colony formation assay **(I)**. **J.** Downregulation of ARRB2 suppresses Enz^R LNCaP cell invasion in a transwell assay. shCtrl or shARRB2 expressing Enz^R LNCaP were seeded in matrigel-coated upper chambers, and invasion were allowed for 2 days. Migrated cells were stained with crystal violet and photographed.
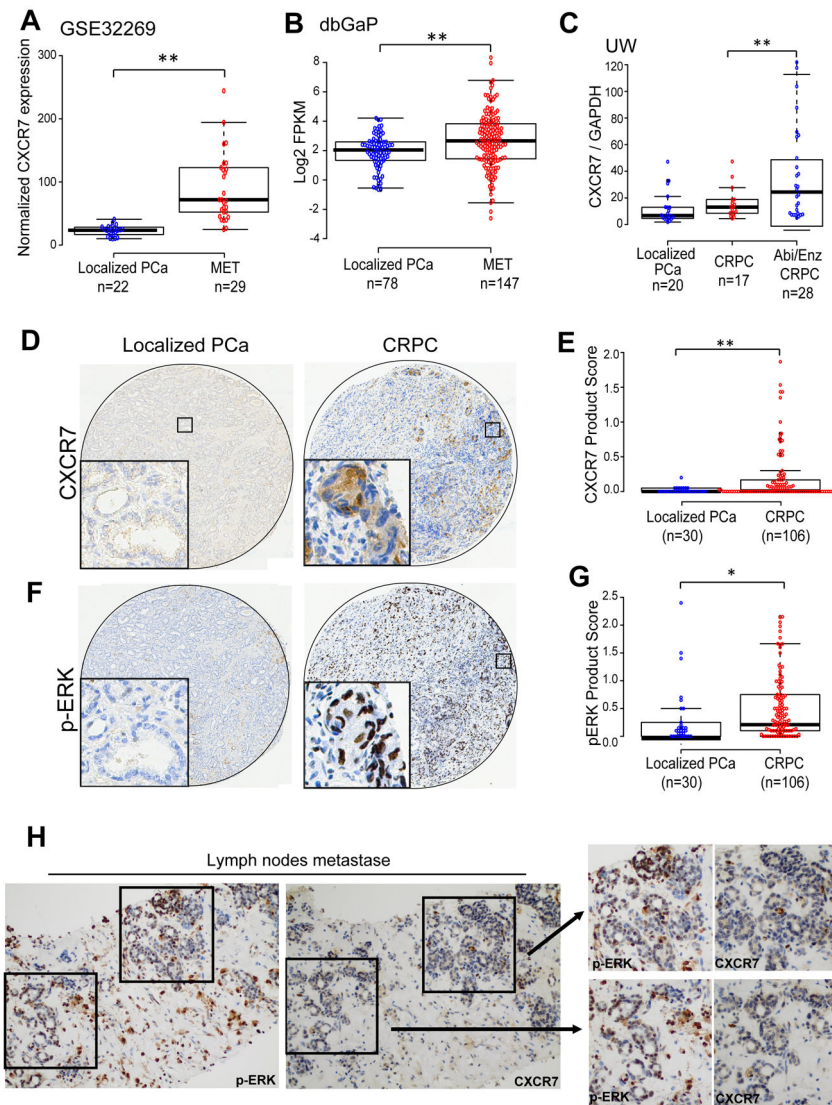
Figure 6. CXCR7 expression is elevated in metastatic CRPC tumors.

A-B. CXCR7 mRNA is upregulated in metastatic prostate tumors. CXCR7 expression in GSE32269 **(A)** and dbGaP (database of Genotypes and Phenotypes) **(B)**. Dataset was comparatively plotted in localized versus metastatic PCa. ** $p<0.01$.

C. CXCR7 expression is elevated in CRPC after Abi/Enz treatment. QRT-PCR was performed in a set of localized PC, CRPC, and Abi/Enz CRPC tissues. ** $p<0.01$.

D-G. CXCR7 and pERK1/2 level is elevated in CRPC. IHC staining of CXCR7 and pERK1/2 was performed in a set of tissue microarrays composed of localized PC and metastatic CRPC. Representative cases of CXCR7 **(D)** or pERK1/2 **(E)** staining are shown. For each core the percentage of staining and the intensity of staining was scored and the product generated and summarized in boxplots for CXCR7 **(F)** and pERK1/2 **(G)**. * $p<0.05$; ** $p<0.01$.

H. Concordant increases of CXCR7 and pERK1/2 in Enz[R] CRPC with good response to Tra. Metastatic lymph nodes tissues were collected post-Enz but prior to Tra treatment and
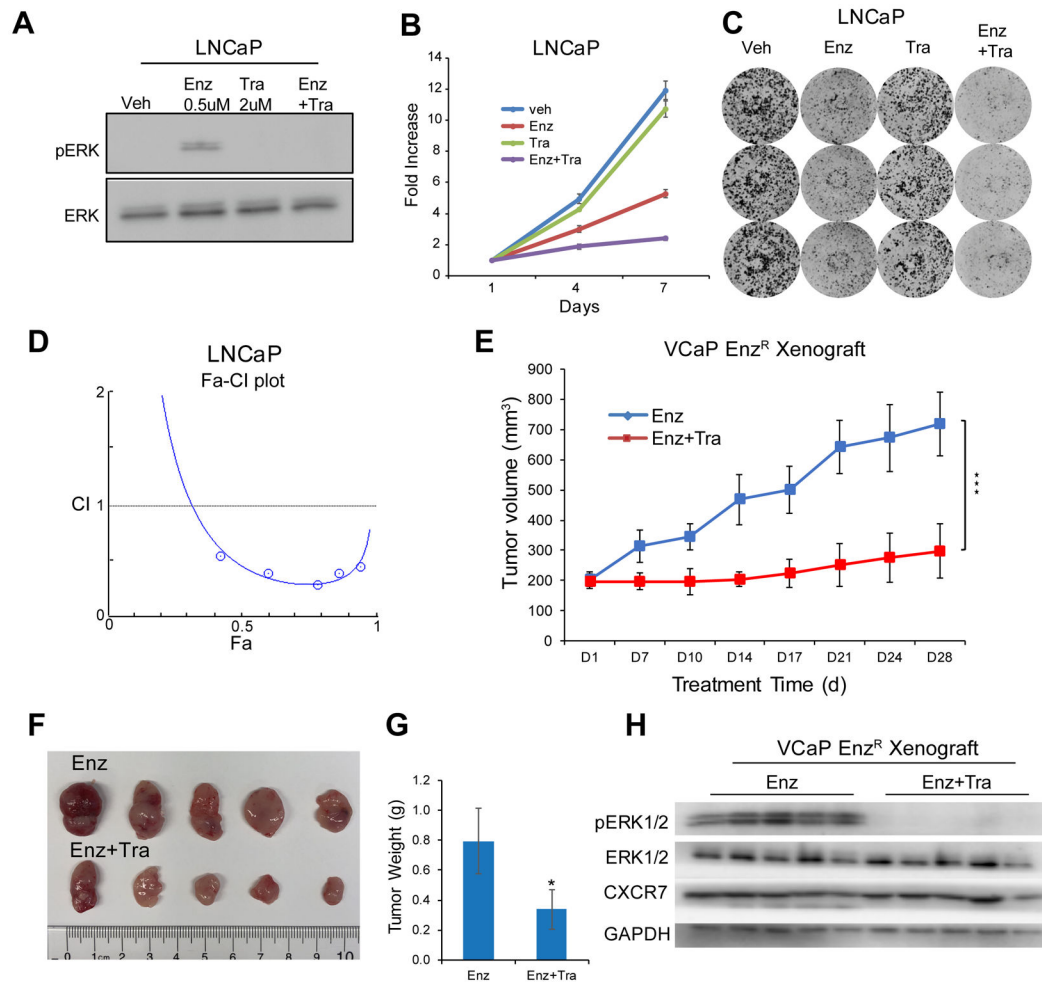
then subjected to IHC staining of CXCR7 and pERK1/2. Representative images were shown and indicated areas were enlarged.

Figure 7. MEK inhibitor trametinib suppresses Enz-resistant prostate cancer growth in *vitro* and *in vivo*.

A. MEK inhibitor blocks MAPK pathway activation. Western blot depicted pERK1/2 protein level in LNCaP cells in response to Veh, Enz (0.5μM), Tra (2μM) and Enz+Tra treatment for 5 days.

B. MAPK pathway inhibitors suppresses PCa cell proliferation. LNCaP cells were treated with Veh, Enz (0.5μM), Tra (2μM) and Enz+Tra and then subjected to WST-1 cell growth assay.

C. MAPK pathway inhibition suppresses anchorage-independent PCa cell growth. LNCaP cells with indicated treatment were seeded in 6-well plates to allow colony formation for 2 weeks. Cell colonies were stained with crystal violet and photographed.

D. Combination of Enz+Tra imposed a synergistic effect on PCa proliferation. WST1 assays were performed using LNCaP cells treated with different doses of Enz (0.25, 0.625, 1.25, 2.5, 5 μM), Tra (1, 2.5, 5, 10, 20μM) or both (ratio of Enz/Tra=1:4). A fraction affected (Fa) vs combination index (CI) plot was generated using the commercial software package CompuSyn. CI<1 represents synergism, CI=1 indicates additive effect and CI>1 represents antagonism.

E-H. Concurrently Tra treatment abolished Enz^R PCa xenograft tumor growth. Enz^R VCaP cells were inoculated into the dorsal flank of nude mice, which were then surgically castrated. Tumor bearing mice were treated with either Enz alone (10mg/kg) or in combination with Tra (3mg/kg) once per day by oral gavage, 5 days per week for a total of 4 weeks. Tumor size was evaluated twice biweekly and compared between groups (ANOVA, ***p<0.001) **(E)**. Representative images from tumors excised from the euthanized mice receiving indicated treatment **(F)**. Tumors excised from the euthanized mice were weighted and compared (T-test *p<0.05) **(G)**. Effect of Tra in abolishing pERK1/2 was confirmed by western blot analysis of protein lysates from xenograft tumor tissues **(H)**.